

High temperature spectroscopy of ensembles of nitrogen vacancy centers in diamond

Mohammed Attrash, Oleg Shtempluck, and Eyal Buks*

Andrew and Erna Viterbi Department of Electrical Engineering, Technion, Haifa 32000 Israel

(Dated: November 21, 2022)

We study spectroscopy of an ensemble of negatively charged nitrogen-vacancy (NV^-) centers in diamond at high temperatures between room temperature and 700 K under high vacuum conditions. Spin resonances are studied using optical detection of magnetic resonance (ODMR), and optical spectroscopy is employed to study radiative transitions. Upon increasing the temperature the intensity of radiative decay in visible and infra-red decreased. In addition, the ODMR resonance frequencies were decreased, and the phonon line emission shifted to higher wavelengths. Density functional theory calculation of the zero-field splitting parameter (D) revealed that thermal expansion is not enough to explain the shift in the ODMR frequencies. Fitting the measured intensity of photo-luminescence with the theoretical predictions of the Mott-Seitz model yields the value of 0.22 eV for the energy barrier associated with nonradiative decay.

I. INTRODUCTION

Negatively charged nitrogen vacancy (NV^-) center in diamond is considered as a candidate for quantum technologies due to its unique physical properties, such as long coherence time at room temperature. The technique of optical detection of magnetic resonance (ODMR) allows monitoring spin resonances [1–4], whereas radiative transitions can be probed using optical spectroscopy. Many researchers investigated the temperature dependence of luminescence of NV [5–9]. It was found that the magnetic resonance frequencies were decreased after increasing the temperature. The shift of the frequency lines is attributed to the temperature dependence of the NV^- zero-field splitting parameter D . This dependency was explained by a combination of two mechanisms, thermal expansion [10] and electron-phonon interactions [8]. It is acclaimed that the non-radiative processes shorten the excited-state lifetime at high temperatures [5, 11, 12]. Beside shift in frequencies, the photo-luminescence (PL) intensity was found to decrease at high temperatures. Two models were proposed to explain PL intensity decay: Mott-Seitz [13, 14] and Schon-Klasens [15–17]. In the Mott-Seitz model, the PL quenching at high temperature is due to the enhancement of the non-radiative process. On the other hand, in the Schon-Klasens model, the PL decreases due to radiationless recombination of holes and electrons at non-radiative recombination centers. Despite the extensive studies of the NV at high temperatures, some remaining issues were not thoroughly investigated.

In this work we employ both ODMR in the microwave (MW) band, and optical spectroscopy in the optical band of 500 – 1500 nm, to study ensembles of NV^- centers in a high vacuum (HV) system at different temperatures (300–550 K). The comparison between our experimental results and theory yields partial agreement.

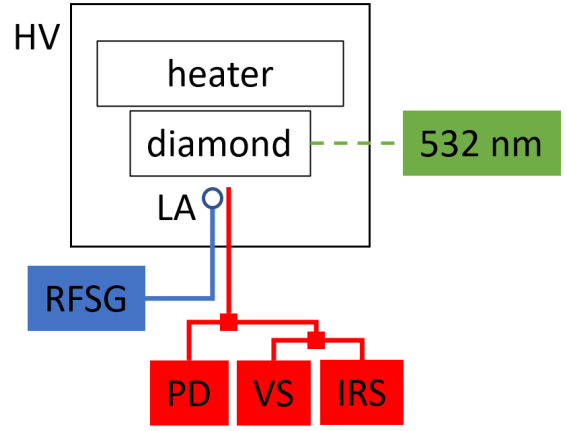


FIG. 1: Experimental setup. The diamond wafer is attached to a heater stage inside the HV chamber. Both a MW LA and a multi-mode optical fiber are attached to a copper-made finger cooled by liquid nitrogen. The optical fiber is split to 3 components, which are connected to the PD, VS and IRS. The NV^- is excited by a 532 nm laser delivered via free space. The optical propagation direction is parallel to the [110] plane. The magnetic field is applied by a cylindrical neodymium magnet.

II. EXPERIMENTAL SETUP

Type Ib high pressure high temperature (HPHT) single crystal diamond with a nitrogen concentration lower than 200 ppm was laser-cut along the [110] plane, polished and irradiated with 2.8 MeV electrons at a dose of $8 \times 10^{18} \text{ cm}^{-2}$, and annealed at 900°C for 2 hours. The estimated NV^- concentration is $3.3 \times 10^{17} \text{ cm}^{-3}$ [20]. The diamond was cleaned in an acid mixture of Perchloric, Sulfuric, and Fuming Nitric acid for 1 hour.

The experimental setup is schematically shown in Fig. 1. The vacuum system, which has a base pressure of 1×10^{-6} Torr, includes an ultra HV heater (HeatWave Labs Inc., model 101491) connected to a thermocouple (type K) and a temperature controller (model 101303),

*corresponding author: eyal@ee.technion.ac.il

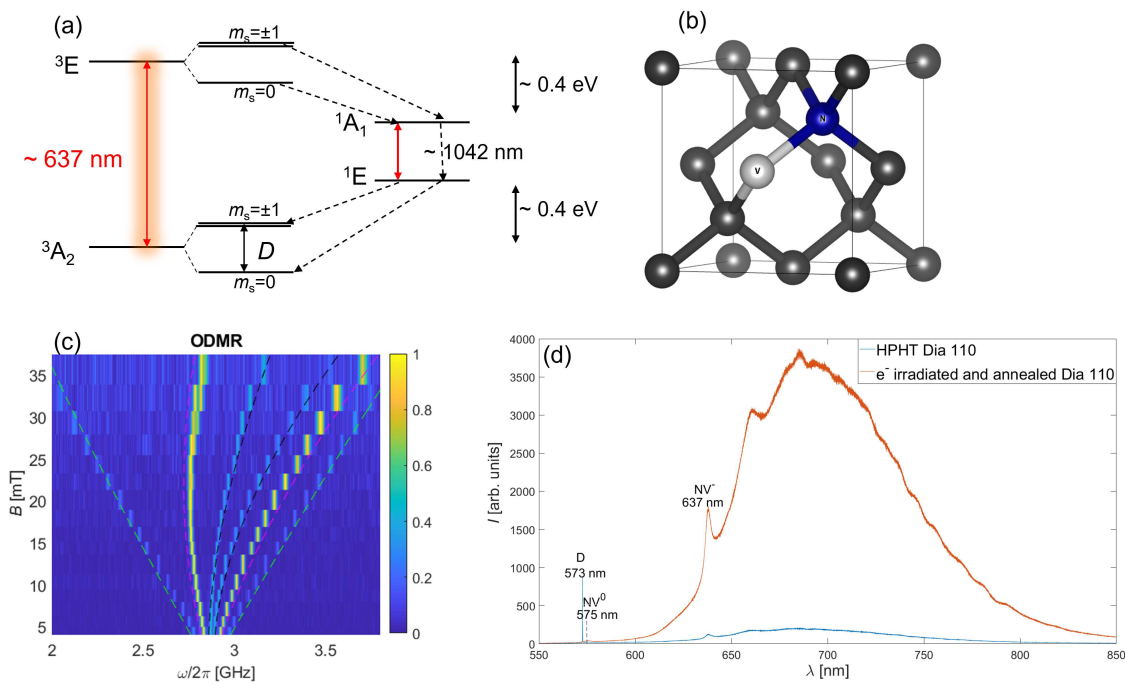


FIG. 2: (a) Schematics of the NV^- electronic structure, the $^3\text{A}_2$ and ^3E are the triplet ground and excited states, respectively, while $^1\text{A}_1$ and ^1E are singlet states, which involved in the intersystem crossing. The solid lines represent the optical transitions, while the dashed lines represent the non-radiative transitions. (b) NV unit cell structure, where carbon atoms are in gray, nitrogen in blue, and vacancy in white. (c) ODMR plot at room temperature. The color bar indicates the normalized ODMR intensity. The dashed lines represent the resonances related to spin transitions from $m_s = \pm 1$ to $m_s = 0$ for the four different NV^- center directions (the resonances corresponding to two directions are nearly degenerate). (d) PL measurement of HPHT diamond [110] before and after electron irradiation and annealing. For HPHT diamond, two features are observed: at 573 nm, which is related to diamond Raman peak [18, 19], and at 637 nm, which is related to NV^- zero-phonon line. After electron irradiation and annealing, a very low peak intensity at 575 nm can be observed which is related to NV^0 centers in diamond. In addition, the phonon line intensity (600 - 850 nm) increased.

MW loop antenna (LA), and multi-mode optical fiber to measure the PL emitted from the diamond. Liquid nitrogen was flowed in a metal finger attached to the LA and the optical fiber to avoid annealing damage. The optical fiber is split to 3 components, which are connected to: photo-diode (PD) (Thorlabs, PDA100A), visible spectrometer (VS) (Thorlabs, CCS175, 500 – 1000 nm), and infrared spectrometer (IRS) (Ibsen photonics, ROCK NIR 900 – 1700 nm). The relative optical power delivered to the PD, VS and IRS is 0.5, 0.25 and 0.25, respectively. The spectrometers allow monitoring both the triplet-triplet transition at wavelength of 637 nm and the singlet-singlet transition at 1042 nm [see the schematic energy level diagram shown in Fig. 2(a)].

The NV^- centers were excited by a 532 nm green laser delivered via free space. The LA is connected to a radio frequency signal source (RFSG), and the MW amplitude was modulated by a 151 Hz sine wave. The PD is attached to a 600 nm long-pass filter, and its signal was demodulated by a lock-in amplifier. To apply magnetic field on the diamond, a cylindrical neodymium magnet is positioned outside the vacuum chamber using a motorized stage. To reduce laser intensity fluctuations, we

used proportional integral derivative controller (SIM 960 - Stanford Research Systems).

III. ODMR

Ignoring the hyper-fine interaction, the NV^- spin triplet ground state Hamiltonian \mathcal{H}_{NV} is given by

$$\frac{\mathcal{H}_{\text{NV}}}{\hbar} = \frac{D\mathcal{S}_z^2}{\hbar^2} - \frac{\gamma_e \vec{B} \cdot \mathcal{S}}{\hbar} + \frac{E_{\text{NV}} (\mathcal{S}_+^2 + \mathcal{S}_-^2)}{2\hbar^2}, \quad (1)$$

where D and E_{NV} are the zero field splitting parameters, which equal to $2\pi \times 2.88$ GHz and $2\pi \times 10$ MHz at 3.6 K, respectively [20], \mathcal{S} is the total spin operator $\mathcal{S} = \mathcal{S}_x \hat{x} + \mathcal{S}_y \hat{y} + \mathcal{S}_z \hat{z}$, $\gamma_e = 2\pi \times 28.03$ GHz T^{-1} is the electron spin gyromagnetic ratio, \vec{B} is the magnetic field, and $\mathcal{S}_{\pm} = \mathcal{S}_x \pm i\mathcal{S}_y$. Under continuous laser excitation, the NV^- is polarized to the spin state $m_s = 0$, which has a brighter PL [21].

Figure 2(a) shows a schematic energy level diagram of an NV^- center. The structure of nitrogen vacancy center in diamond is shown in Fig. 2(b). Measured ODMR of

our sample as a function of magnetic field is shown in Fig. 2(c). The eight lines that are observed in this figure represent the resonances related to spin transitions from $m_s = \pm 1$ to $m_s = 0$ for the four different NV⁻ center directions. The dashed lines represent the theoretically calculated frequencies of the same resonances, which are obtained by numerically diagonalizing the Hamiltonian \mathcal{H}_{NV} (1). Note that two pairs of resonances, which are represented by the pink dash lines, are nearly degenerate (note that their ODMR signal is nearly double the signal of the other NV directions). Figure 2(d) reveals the PL measurement of the HPHT diamond sample before and after electron irradiation and annealing. The measurement was recorded by Micro-Raman spectrometer (LABRAM HR, HORIBA, Jobin Yvon) using 532 nm wavelength laser at room temperature (laser power was lower than 10 mW). The HPHT diamond reveals a peak at 573 nm related to diamond Raman peak [18, 19], and another low intensity peak at 637 nm that is related to the zero phonon line of NV⁻ [see Fig. 2(a)] [22, 23]. After electron irradiation and annealing process, the intensity of NV⁻ zero phonon line increased, beside the PL intensity increase in the entire range of 650 – 850 nm. The intensity of the NV⁰ zero phonon line is very low in the treated diamond sample. The reason for relatively low NV⁰ peak intensity may be related to low laser power, as was found in Ref. [24].

IV. ZERO FIELD SPLITTING D

To numerically investigate the shift in the zero field splitting D , density functional theory (DFT) [26, 27] was used as implemented in the QUANTUM ESPRESSO software [28]. The defect structure was modeled with $3 \times 3 \times 2$ and $2 \times 2 \times 2$ super-cell of diamond (144 and 64 atoms, respectively) and Γ point sampling of Brillouin zone. The calculation were performed with projector augmented-wave (PAW) method [29] and Perdew-Burke-Ernzerhof (PBE) exchange-correlation functional [30] with a plane-wave cutoff of 300 Ry. To investigate the thermal expansion effect on D , the lattice length of the structure was chosen to suit the temperature as found in previous experiments [31, 32], and the structure was relaxed at constant lattice length until the total force on the atoms was lower than $26 \times 10^{-3} \text{ eV \AA}^{-1}$. The zero field splitting D is believed to be related to spin-spin interactions of unpaired electrons [33]. Its tensor components D_{ab} are given by [34]

$$D_{ab} = \frac{(\gamma_e \hbar)^2}{2S(2S-1)} \frac{\mu_0}{4\pi} \times \sum_{i < j} \chi_{ij} \langle \psi_{ij} | \frac{r^2 \delta_{ab} - 3r_a r_b}{r^5} | \psi_{ij} \rangle, \quad (2)$$

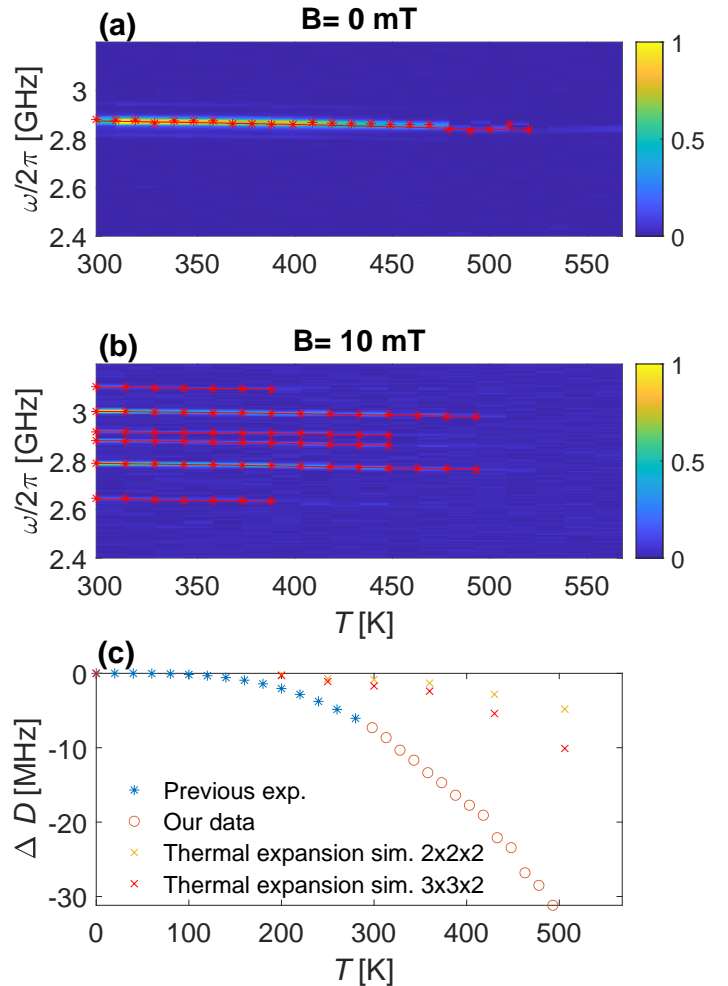


FIG. 3: (a) and (b) ODMR as a function of temperature recorded at magnetic field of 0 and 10 mT, respectively. The ODMR frequencies decrease as temperature increases due to the decrease of D . Fitting of D was done according to the parameters presented in Ref. [5]. (c) The shift ΔD in D as a function of temperature. Note that D is assumed to be independent on the externally applied magnetic field for all fitting lines in (a) and (b). The previous experimental data [see blue stars in (c)] are from [8, 25].

where $a, b \in \{x, y, z\}$ are Cartesian indices, μ_0 is the magnetic permeability of free space, the summation includes all pairs of occupied Kohn-Sham orbitals, $\chi_{ij} = \pm 1$ for parallel and anti-parallel spins, respectively, S is the spin number, and $\psi_{ij}(r, r')$ is 2×2 determinant which can be written as $\psi_{ij}(r, r') = 2^{-1/2}[\psi_i(r)\psi_j(r') - \psi_i(r')\psi_j(r)]$. A Python package named PyZFS was used to calculate D_{ab} [35].

According to our DFT calculations, the D at zero temperature equals to 2.84 GHz for $3 \times 3 \times 2$ super-cell (2.77 GHz for $2 \times 2 \times 2$ super-cell) while the experimental value at 3.6 K equals to 2.88 GHz. For comparison to other DFT results, D was found in the range of [2.7, 3] GHz [36–38]. The shift of D at a given tempera-

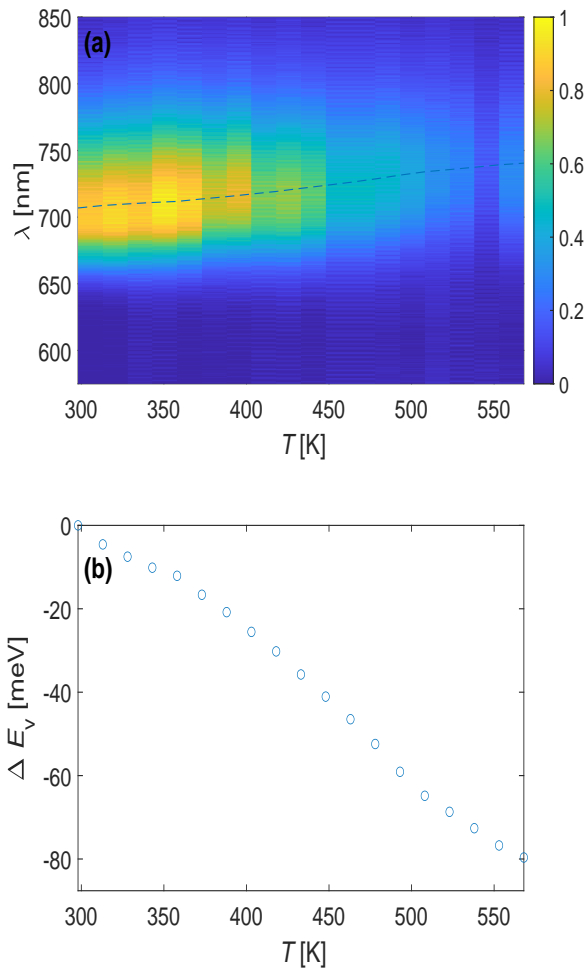


FIG. 4: (a) Optical emission spectra of NV^- at different temperatures. The peak intensity shifted to higher wavelength at increased temperatures. (b) Peak shift ΔE_V as a function of the temperature T .

ture, relative to its value at zero temperature, is denoted by ΔD . Some studies calculated the shift ΔD according to the thermal expansion at temperatures below 300 K [8, 10]. To account for our experimental results, we calculate ΔD based on the thermal expansion in the range from absolute zero to 500 K.

In order to investigate the temperature effect on the ODMR, the diamond was annealed at different temperatures under constant magnetic field. The ODMR at temperatures below 520 K [see Fig 3(a)] reveals resonance lines related to NV^- . Upon increasing the temperature, the resonance frequencies and their intensity were decreased, and above 520 K the resonance lines could not be resolved. It is expected that the shift in resonance lines is due to the decrease of D . The measured shift ΔD in D [see Fig. 3(b)] at 500 K equals to -32 MHz and the slope dD/dT is of order of -100 kHz K^{-1} , in agreement with the value reported in [5]. The normalized slope $d \log D/dT$ is $-4.3 \times 10^{-5} \text{ K}^{-1}$, which is higher

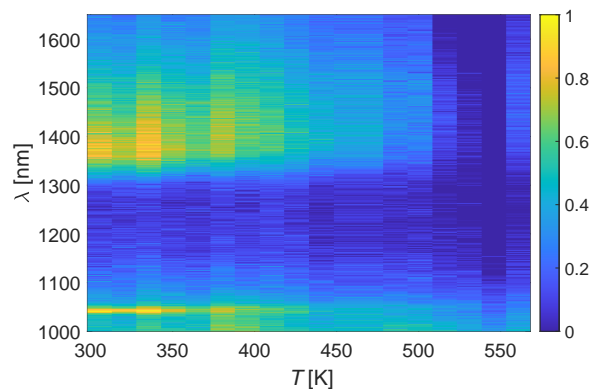


FIG. 5: IR emission as a function of temperature T and wavelength λ . The peak at 1042 nm, which represent the radiative decay in the intermediate singlet states ${}^1\text{A}_1 \rightarrow {}^1\text{E}$, can be observed at temperatures below 450 K.

than what was found in experiments carried out at lower temperatures, for which the value of $-2.61 \times 10^{-5} \text{ K}^{-1}$ has been measured [7, 9].

The experimental results of D at temperatures lower than 300 K were taken from other reports [7, 8]. As can be observed from simulation results, D decreases as the temperature increases. The shift in D at 500 K compare to its value at 300 K according to our calculations is -10 MHz (-4 MHz for the $2 \times 2 \times 2$ super-cell). As can be seen from the plot in Fig. 3(b), the thermal expansion is not enough to explain the shift in D . The unit cell length a of diamond at 298 K and 506 K equals to 3.5668 \AA and 3.5680 \AA , respectively [31], therefore, $d \log a/dT \simeq 1.6 \times 10^{-6} \text{ K}^{-1}$ in this range. This value is too small to account for the above-mentioned experimental finding that $d \log D/dT$ is $-4.3 \times 10^{-5} \text{ K}^{-1}$ in the same range.

According to a first-principles calculation reported in [39], the shift in D at 500 K is -18 MHz, while the shift in our data is -32 MHz. Good agreement is found between our experimental results, and the ones reported in Ref. [5], in which the zero-field splitting parameter D is expressed as a a power series of the temperature T .

The ODMR signal intensity can be derived from the rate equation that governs the time evolution of the spin polarization (see appendix A of Ref. [20]). As can be seen from Fig. 3, ODMR signals could not be experimentally resolved above a temperature of about 520 K. On the other hand, PL signals were measured at higher temperatures up to about 700 K (see Fig. 6). This observation suggests that the dominant mechanism responsible for the observed ODMR signal drop with temperature [see Fig. 3(a)], is dephasing, which enhances spin transverse relaxation, and consequently disables ODMR above 520 K.

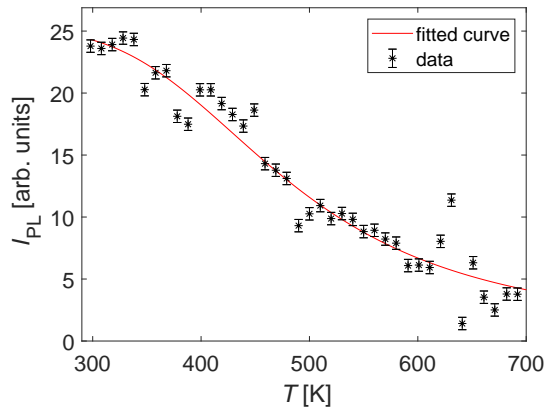


FIG. 6: PL intensity I_{PL} as a function of temperature T . The red solid line is calculated using Eq. (3).

V. OPTICAL SPECTROSCOPY

The fluorescence emission spectra of NV^- (measured by the VS) at different temperatures is shown in Fig. 4. The fluorescence can be resolved at temperatures up to 520 K. The spectra is shifted to higher wavelengths at higher temperatures. The shift in wavelength at which the emission intensity is maximized, which is denoted by λ_{max} , equals to $hc/60 \text{ meV}$ at 500 K, where h is the Planck constant and c is the speed of light, and thus $d \log \lambda_{\text{max}}/dT \simeq 3.1 \times 10^{-4} \text{ K}^{-1}$.

The IR spectra of the NV^- ensemble (measured by the IRS) at different temperatures is shown in Fig. 5. The peak at 1042 nm, which is associated with radiation decay from the ${}^1\text{A}_1$ to E_1 levels [see Fig.2(a)], is observed at room temperatures. Upon heating the diamond, the 1042 nm peak intensity decreased and became unresolved at temperatures above 450 K. Temperature dependence of the ${}^1\text{A}_1$ to E_1 transition wavelength has been observed in [8]. However, this dependency cannot be resolved in our measurements due to limited IRS resolution. Another feature can be observed at 1350 nm, which is related to second order phonon line (note that $1350/2 = 675$). This feature can be suppressed by adding a 900 nm long pass filter. The singlet NV^- transition (from ${}^1\text{A}_1$ to E_1

states) wavelength is found to be less sensitive to temperature compare to the triplet transition (from ${}^3\text{A}_2$ to ${}^3\text{E}$ states) wavelength.

Finally, we discuss the PL intensity and energy barrier for the nonradiative process, which is denoted by U_{b} . The PL intensity I_{PL} as a function of the temperature T is shown in Fig. 6. In the Mott-Seitz model this dependency of I_{PL} on T is given by [see Eq. (2) of Ref. [40], and Eq. (5) of Ref. [41]]

$$I_{\text{PL}} = \frac{I_0}{1 + C \exp\left(-\frac{U_{\text{b}}}{k_{\text{B}}T}\right)}, \quad (3)$$

where I_0 is the zero temperature intensity, C is a constant, and k_{B} is the Boltzmann's constant. Fitting the measured PL intensity I_{PL} with Eq. (3) yields $U_{\text{b}} = 0.22 \pm 0.05 \text{ eV}$ and $C = 200$. Note that U_{b} was found in ref. [5] to be 0.48 eV. The deviation between this result [5], which was obtained with a single NV^- center, and our extracted value for the energetic barrier, can perhaps be attributed to impurities near the single NV center that was studied in Ref. [5]. The effect of nearby impurities on coherence lifetime of NV^- centers has been studied in [42].

VI. SUMMARY

In this study we investigated the optical properties of an ensemble of NV^- centers in diamond as a function of temperature. The NV^- emission in the visible ($\sim 700 \text{ nm}$) and IR ($\sim 1042 \text{ nm}$) regions decreased upon increasing the temperature, and the phonon line wavelength at maximum intensity of the NV^- (650 – 800 nm) increased. The D parameter decreased upon increasing the temperature, and the thermal expansion model is not enough to explain this behaviour. By applying the Mott-Seitz model we find that the energy barrier for nonradiative decay U_{b} is in the range $[0.17, 0.27] \text{ eV}$.

This work was supported by the Israeli science foundation, the Israeli ministry of science, and by the Technion security research foundation. We would like to thank Prof. Joan Adler, Department of Physics - Technion, for providing computational facilities.

-
- [1] A Gruber, A Dräbenstedt, C Tietz, L Fleury, J Wrachtrup, and C Von Borczyskowski, “Scanning confocal optical microscopy and magnetic resonance on single defect centers”, *Science*, vol. 276, no. 5321, pp. 2012–2014, 1997.
- [2] Thomas Wolf, Philipp Neumann, Kazuo Nakamura, Hitoshi Sumiya, Takeshi Ohshima, Junichi Isoya, and Jörg Wrachtrup, “Subpicotesla diamond magnetometry”, *Physical Review X*, vol. 5, no. 4, pp. 041001, 2015.
- [3] Dominik M. Juraschek, Quintin N. Meier, Morgan

- Trassin, Susan E. Trolier-McKinstry, Christian L. Degen, and Nicola A. Spaldin, “Dynamical magnetic field accompanying the motion of ferroelectric domain walls”, *Phys. Rev. Lett.*, vol. 123, pp. 127601, Sep 2019.
- [4] Dinesh Pinto, Domenico Paone, Bastian Kern, Tim Dierker, René Wiczorek, Aparajita Singha, Durga Dasari, Amit Finkler, Wolfgang Harneit, Jörg Wrachtrup, et al., “Readout and control of an endofullerene electronic spin”, *Nature communications*, vol. 11, no. 1, pp. 1–6, 2020.

- [5] D. M. Toyli, D. J. Christle, A. Alkauskas, B. B. Buckley, C. G. Van de Walle, and D. D. Awschalom, “Measurement and control of single nitrogen-vacancy center spins above 600 k”, *Phys. Rev. X*, vol. 2, pp. 031001, Jul 2012.
- [6] A. T. Collins, M. F. Thomaz, and M. I. B. Jorge, “Luminescence decay time of the 1.945 eV centre in type Ib diamond”, *Journal of Physics C Solid State Physics*, vol. 16, no. 11, pp. 2177–2181, April 1983.
- [7] X.-D. Chen, C.-H. Dong, F.-W. Sun, C.-L. Zou, J.-M. Cui, Z.-F. Han, and G.-C. Guo, “Temperature dependent energy level shifts of nitrogen-vacancy centers in diamond”, *Applied Physics Letters*, vol. 99, no. 16, pp. 161903, 2011.
- [8] M. W. Doherty, V. M. Acosta, A. Jarmola, M. S. J. Barson, N. B. Manson, D. Budker, and L. C. L. Hollenberg, “Temperature shifts of the resonances of the nv^- center in diamond”, *Phys. Rev. B*, vol. 90, pp. 041201, Jul 2014.
- [9] V. M. Acosta, E. Bauch, M. P. Ledbetter, A. Waxman, L.-S. Bouchard, and D. Budker, “Temperature dependence of the nitrogen-vacancy magnetic resonance in diamond”, *Phys. Rev. Lett.*, vol. 104, pp. 070801, Feb 2010.
- [10] Viktor Ivády, Tamás Simon, Jeronimo R. Maze, I. A. Abrikosov, and Adam Gali, “Pressure and temperature dependence of the zero-field splitting in the ground state of nv centers in diamond: A first-principles study”, *Phys. Rev. B*, vol. 90, pp. 235205, Dec 2014.
- [11] Taras Plakhotnik and Daniel Gruber, “Luminescence of nitrogen-vacancy centers in nanodiamonds at temperatures between 300 and 700 k: perspectives on nanothermometry”, *Phys. Chem. Chem. Phys.*, vol. 12, pp. 9751–9756, 2010.
- [12] V. M. Acosta, A. Jarmola, E. Bauch, and D. Budker, “Optical properties of the nitrogen-vacancy singlet levels in diamond”, *Phys. Rev. B*, vol. 82, pp. 201202, Nov 2010.
- [13] R. W. Gurney and N. F. Mott, “Luminescence in solids”, *Trans. Faraday Soc.*, vol. 35, pp. 69–73, 1939.
- [14] Frederick Seitz, “An interpretation of crystal luminescence”, *Trans. Faraday Soc.*, vol. 35, pp. 74–85, 1939.
- [15] Michael Schön, “Zum leuchtmechanismus der kristallphosphore”, *Zeitschrift für Physik*, vol. 119, no. 7, pp. 463–471, 1942.
- [16] M. E. Wise and H. A. Klasens, “Fluorescence efficiency and hole migration in zinc sulphides”, *J. Opt. Soc. Am.*, vol. 38, no. 3, pp. 226–231, Mar 1948.
- [17] H. Klasens, “Transfer of energy between centres in zinc sulphide phosphors”, *Nature*, vol. 158, pp. 306–307, 1946.
- [18] Richard P Mildren, James E Butler, and James R Rabeau, “Cvd-diamond external cavity raman laser at 573 nm”, *Optics express*, vol. 16, no. 23, pp. 18950–18955, 2008.
- [19] Maneesh Chandran, Shaul Michaelson, Cecile Saguy, and Alon Hoffman, “Fabrication of a nanometer thick nitrogen delta doped layer at the sub-surface region of (100) diamond”, *Applied Physics Letters*, vol. 109, no. 22, pp. 221602, 2016.
- [20] Nir Alfasi, Sergei Masis, Oleg Shtempluck, and Eyal Buks, “Detection of paramagnetic defects in diamond using off-resonance excitation of nv centers”, *Phys. Rev. B*, vol. 99, pp. 214111, Jun 2019.
- [21] Marcus W Doherty, Neil B Manson, Paul Delaney, Fedor Jelezko, Jörg Wrachtrup, and Lloyd CL Hollenberg, “The nitrogen-vacancy colour centre in diamond”, *Physics Reports*, vol. 528, no. 1, pp. 1–45, 2013.
- [22] Steven Prawer and Robert J Nemanich, “Raman spectroscopy of diamond and doped diamond”, *Philosophical Transactions of the Royal Society of London. Series A: Mathematical, Physical and Engineering Sciences*, vol. 362, no. 1824, pp. 2537–2565, 2004.
- [23] L. Rondin, G. Dantelle, A. Slablab, F. Grosshans, F. Treussart, P. Bergonzo, S. Perruchas, T. Gacoin, M. Chaigneau, H.-C. Chang, V. Jacques, and J.-F. Roch, “Surface-induced charge state conversion of nitrogen-vacancy defects in nanodiamonds”, *Phys. Rev. B*, vol. 82, pp. 115449, Sep 2010.
- [24] NB Manson and JP Harrison, “Photo-ionization of the nitrogen-vacancy center in diamond”, *Diamond and related materials*, vol. 14, no. 10, pp. 1705–1710, 2005.
- [25] AV Feshchenko, O-P Saira, and JP Pekola, “Thermal conductance of nb thin films at sub-kelvin temperatures”, *arXiv:1609.06519*, 2016.
- [26] P. Hohenberg and W. Kohn, “Inhomogeneous electron gas”, *Phys. Rev.*, vol. 136, pp. B864–B871, Nov 1964.
- [27] W. Kohn and L. J. Sham, “Self-consistent equations including exchange and correlation effects”, *Phys. Rev.*, vol. 140, pp. A1133–A1138, Nov 1965.
- [28] Paolo Giannozzi, Stefano Baroni, Nicola Bonini, Matteo Calandra, Roberto Car, Carlo Cavazzoni, Davide Ceresoli, Guido L Chiarotti, Matteo Cococcioni, Ismaila Dabo, Andrea Dal Corso, Stefano de Gironcoli, Stefano Fabris, Guido Fratesi, Ralph Gebauer, Uwe Gerstmann, Christos Gougoussis, Anton Kokalj, Michele Lazzeri, Layla Martin-Samos, Nicola Marzari, Francesco Mauri, Riccardo Mazzarello, Stefano Paolini, Alfredo Pasquarello, Lorenzo Paulatto, Carlo Sbraccia, Sandro Scandolo, Gabriele Sciauzero, Ari P Seitsonen, Alexander Smogunov, Paolo Umari, and Renata M Wentzcovitch, “QUANTUM ESPRESSO: a modular and open-source software project for quantum simulations of materials”, *Journal of Physics: Condensed Matter*, vol. 21, no. 39, pp. 395502, sep 2009.
- [29] P. E. Blöchl, “Projector augmented-wave method”, *Phys. Rev. B*, vol. 50, pp. 17953–17979, Dec 1994.
- [30] John P. Perdew, Kieron Burke, and Matthias Ernzerhof, “Generalized gradient approximation made simple”, *Phys. Rev. Lett.*, vol. 77, pp. 3865–3868, Oct 1996.
- [31] Brian J. Skinner, “The Thermal Expansions of Thoria, Periclase and Diamond*”, *American Mineralogist*, vol. 42, no. 1-2, pp. 39–55, 02 1957.
- [32] Toshimaro Sato, Kazutoshi Ohashi, Tomoko Sudoh, Katsuji Haruna, and Hiroshi Maeta, “Thermal expansion of a high purity synthetic diamond single crystal at low temperatures”, *Phys. Rev. B*, vol. 65, pp. 092102, Feb 2002.
- [33] A. Lenef and S. C. Rand, “Electronic structure of the $n-v$ center in diamond: Theory”, *Phys. Rev. B*, vol. 53, pp. 13441–13455, May 1996.
- [34] John E Harriman, *Theoretical foundations of electron spin resonance: physical chemistry: a series of monographs*, Academic press, 1978.
- [35] He Ma, Marco Govoni, and Giulia Galli, “Pyzfs: A python package for first-principles calculations of zero-field splitting tensors”, *Journal of Open Source Software*, vol. 5, no. 47, pp. 2160, 2020.
- [36] Churna Bhandari, Aleksander L. Wysocki, Sophia E. Economou, Pratibha Dev, and Kyungwha Park, “Multi-configurational study of the negatively charged nitrogen-vacancy center in diamond”, *Phys. Rev. B*, vol. 103, pp.

- 014115, Jan 2021.
- [37] Samuel J Whiteley, Gary Wolfowicz, Christopher P Anderson, Alexandre Bourassa, He Ma, Meng Ye, Gerwin Koolstra, Kevin J Satzinger, Martin V Holt, F Joseph Heremans, et al., “Spin–phonon interactions in silicon carbide addressed by gaussian acoustics”, *Nature Physics*, vol. 15, no. 5, pp. 490–495, 2019.
- [38] Krishnendu Ghosh, He Ma, Vikram Gavini, and Giulia Galli, “All-electron density functional calculations for electron and nuclear spin interactions in molecules and solids”, *Phys. Rev. Materials*, vol. 3, pp. 043801, Apr 2019.
- [39] Hao Tang, Ariel Rebekah Barr, Guoqing Wang, Paola Cappellaro, and Ju Li, “First-principles calculation of the temperature-dependent transition energies in spin defects”, 2022.
- [40] M. S. Akselrod, N. Agersnap Larsen, V. Whitley, and S. W. S. McKeever, “Thermal quenching of f-center luminescence in $\text{Al}_2\text{O}_3:\text{C}$ ”, *Journal of Applied Physics*, vol. 84, no. 6, pp. 3364–3373, 1998.
- [41] M L Chithambo, “The analysis of time-resolved optically stimulated luminescence: II. computer simulations and experimental results”, *Journal of Physics D: Applied Physics*, vol. 40, no. 7, pp. 1880–1889, mar 2007.
- [42] JR Maze, PL Stanwix, JS Hodges, S Hong, JM Taylor, P Cappellaro, L Jiang, MV Gurudev Dutt, E Togan, AS Zibrov, et al., “Nanoscale magnetic sensing with an individual electronic spin in diamond”, *Nature*, vol. 455, no. 7213, pp. 644–647, 2008.